ISCI, Volume *11*

Supplemental Information

Exercise Training Induces Depot-Specific Adaptations to White and Brown Adipose Tissue

Adam C. Lehnig, Revati S. Dewal, Lisa A. Baer, Kathryn M. Kitching, Vitor Rosetto Munoz, Peter J. Arts, Devin A. Sindeldecker, Francis J. May, Hans P.M.M. Lauritzen, Laurie J. Goodyear, and Kristin I. Stanford

Figure S1. Effects of exercise on gene expression in isWAT, Related to Figure 2,3. Expression of genes involved in (A) mitochondrial activity and beiging, (B) glucose metabolism, and (C) fatty acid oxidation in isWAT. Data are presented as means ± S.E.M. (n=8/group; **P*<0.05).

Figure S2. Effects of exercise on gene expression in cWAT and rpWAT, Related to Figure 4-6. Expression of genes involved in mitochondrial activity and beiging, glucose metabolism, and fatty acid oxidation in cWAT (A-C) and rpWAT (D-F). Data are presented as means ± S.E.M. (n=8/group; **P*<0.05; ***P*<0.01).

Figure S3. Effects of exercise on triWAT, Related to Figure 4-6. (A) Expression of genes involved in mitochondrial activity and beiging, (B) glucose metabolism, and (C) fatty acid oxidation in triWAT. Protein expression of (D) CS, (E) HK2, (F) GLUT1, (G) GLUT4, (H) CD36, (I) FATP1, and (J) pHSL/HSL in triWAT. Data are presented as means ± S.E.M. (n=8/group).

Figure S4. Effects of exercise on gene expression in mBAT, prBAT, aBAT, and cBAT, Relate to Figure 7. Expression of genes involved in mitochondrial activity and beiging, glucose metabolism, and fatty acid oxidation in mBAT (A-C), prBAT (D-F), aBAT (G-I), and cBAT (J-L). Data are presented as means ± S.E.M. (n=8/group; **P*<0.05, ***P*<0.01).

Figure S1

A

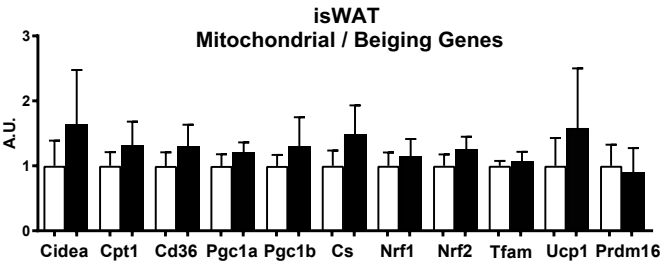

B

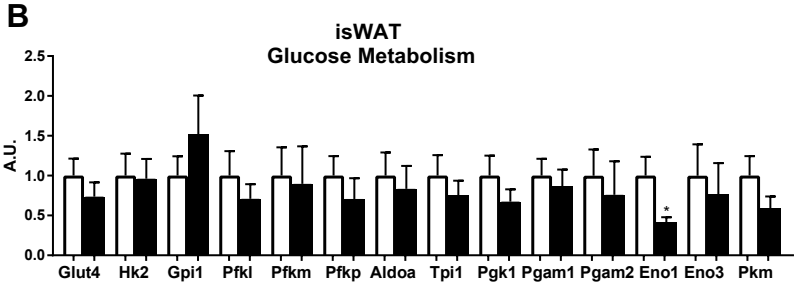

C

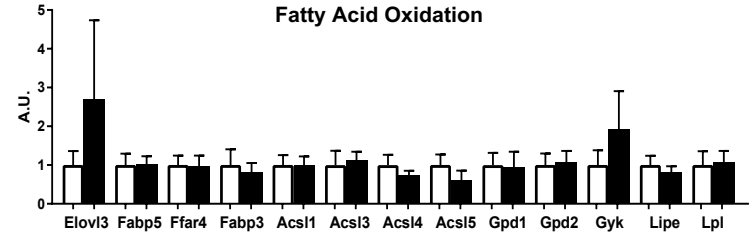

Figure S2

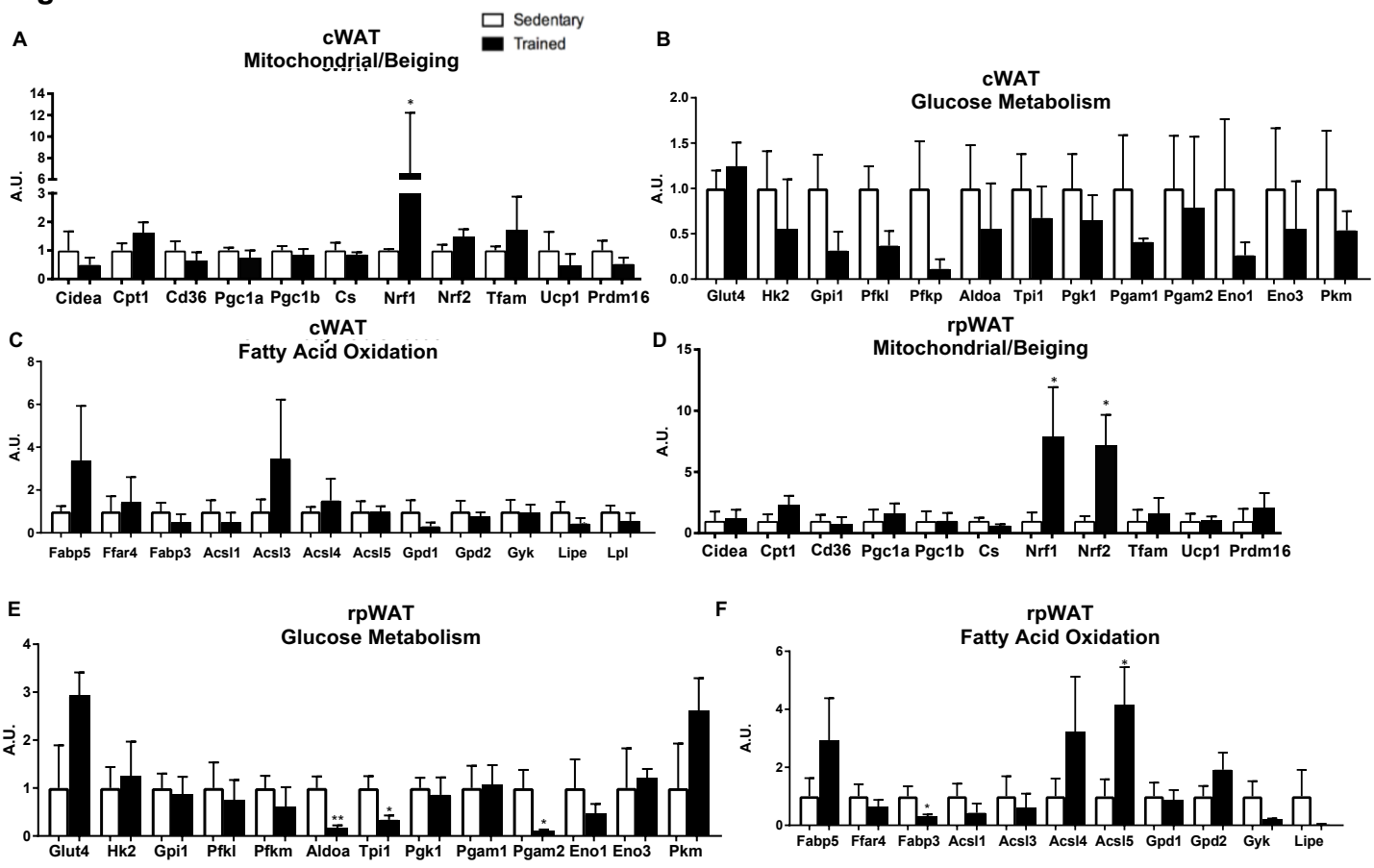
A
cWAT
Mitochondrial/Beiging
Sedentary
Trained
A.U.
Cidea
Cpt1
Cd36
Pgc1a
Pgc1b
Cs
Nrf1
Nrf2
Tfam
Ucp1
Prdm16
B
cWAT
Glucose Metabolism
A.U.
Glut4
Hk2
Gpi1
Pfkl
Pfkp
Aldoa
Tpi1
Pgk1
Pgam1
Pgam2
Eno1
Eno3
Pkm
C
cWAT
Fatty Acid Oxidation
A.U.
Fabp5
Ffar4
Fabp3
Acsl1
Acsl3
Acsl4
Acsl5
Gpd1
Gpd2
Gyk
Lipe
Lpl
D
rpWAT
Mitochondrial/Beiging
A.U.
Cidea
Cpt1
Cd36
Pgc1a
Pgc1b
Cs
Nrf1
Nrf2
Tfam
Ucp1
Prdm16
E
rpWAT
Glucose Metabolism
A.U.
Glut4
Hk2
Gpi1
Pfkl
Pfkm
Aldoa
Tpi1
Pgk1
Pgam1
Pgam2
Eno1
Eno3
Pkm
F
rpWAT
Fatty Acid Oxidation
A.U.
Fabp5
Ffar4
Fabp3
Acsl1
Acsl3
Acsl4
Acsl5
Gpd1
Gpd2
Gyk
Lipe

Figure S3

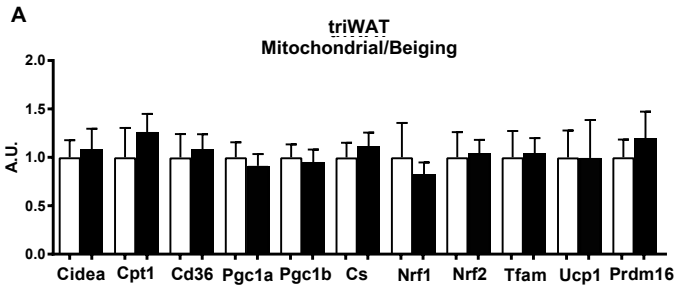
A
triWAT
Mitochondrial/Beiging
A.U.
2.0
1.5
1.0
0.5
0.0
Cidea
Cpt1
Cd36
Pgc1a
Pgc1b
Cs
Nrf1
Nrf2
Tfam
Ucp1
Prdm16

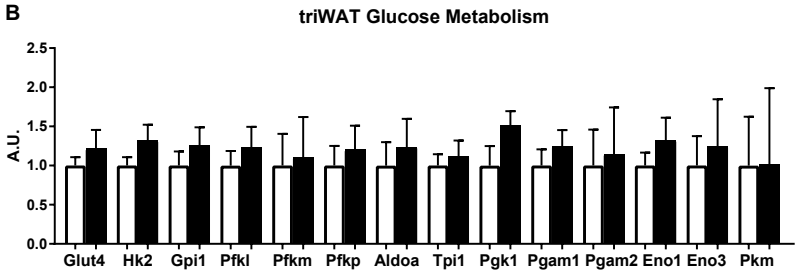
B
triWAT Glucose Metabolism
A.U.
2.5
2.0
1.5
1.0
0.5
0.0
Glut4
Hk2
Gpi1
Pfkl
Pfkm
Pfkp
Aldoa
Tpi1
Pgk1
Pgam1
Pgam2
Eno1
Eno3
Pkm

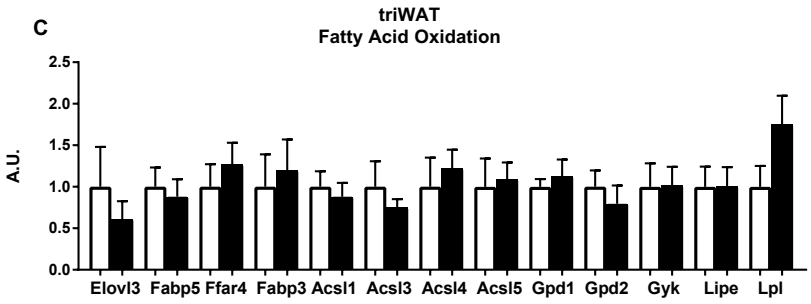
C
triWAT
Fatty Acid Oxidation
A.U.
2.5
2.0
1.5
1.0
0.5
0.0
Elovl3
Fabp5
Ffar4
Fabp3
Acsl1
Acsl3
Acsl4
Acsl5
Gpd1
Gpd2
Gyk
Lipe
Lpl

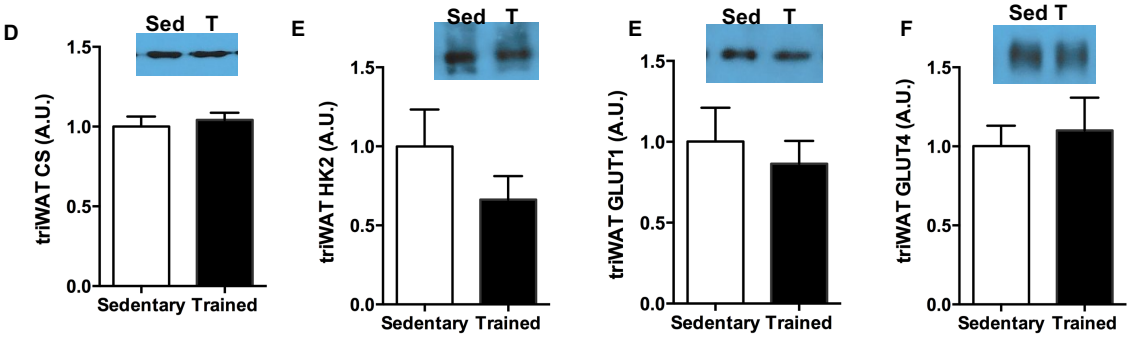
D
Sed
T
triWAT CS (A.U.)
1.5
1.0
0.5
0.0
Sedentary
Trained
E
Sed
T
triWAT HK2 (A.U.)
1.5
1.0
0.5
0.0
Sedentary
Trained
E
Sed
T
triWAT GLUT1 (A.U.)
1.5
1.0
0.5
0.0
Sedentary
Trained
F
Sed
T
triWAT GLUT4 (A.U.)
1.5
1.0
0.5
0.0
Sedentary
Trained

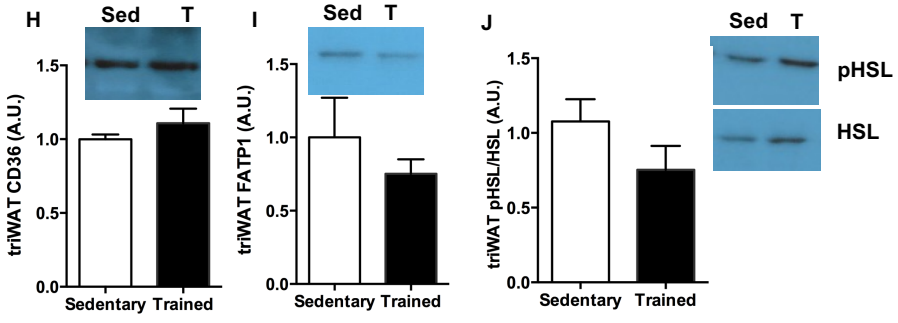
H
Sed
T
triWAT CD36 (A.U.)
1.5
1.0
0.5
0.0
Sedentary
Trained
I
Sed
T
triWAT FATP1 (A.U.)
1.5
1.0
0.5
0.0
Sedentary
Trained
J
Sed
T
pHSL
HSL
triWAT pHSL/HSL (A.U.)
1.5
1.0
0.5
0.0
Sedentary
Trained

Figure S4

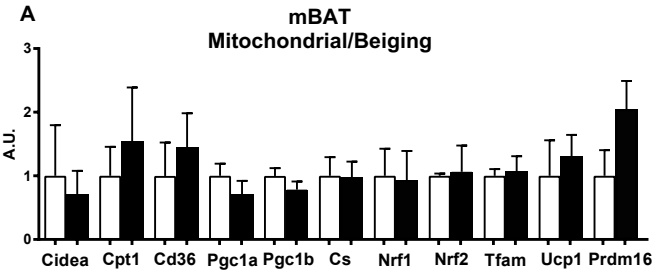
A
mBAT
Mitochondrial/Beiging
A.U.
Cidea Cpt1 Cd36 Pgc1a Pgc1b Cs Nrf1 Nrf2 Tfam Ucp1 Prdm16

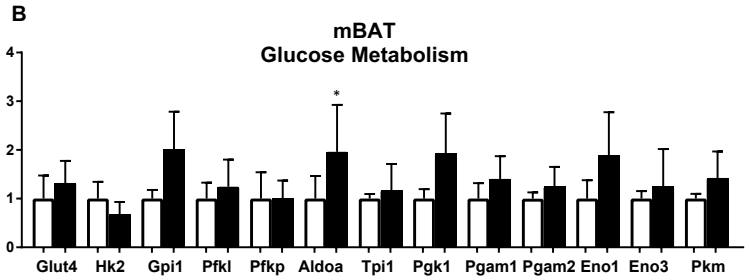
B
mBAT
Glucose Metabolism
A.U.
*
Glut4 Hk2 Gpi1 Pfkl Pfkp Aldoa Tpi1 Pgk1 Pgam1 Pgam2 Eno1 Eno3 Pkm

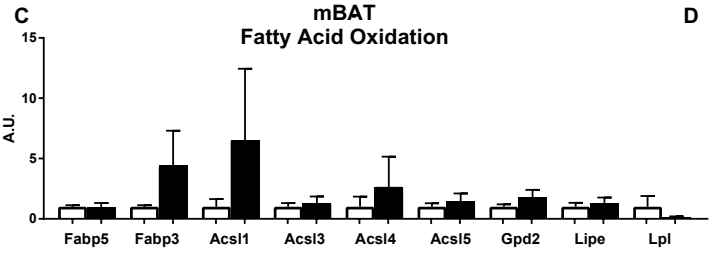
C
mBAT
Fatty Acid Oxidation
A.U.
Fabp5 Fabp3 Acsl1 Acsl3 Acsl4 Acsl5 Gpd2 Lipe Lpl

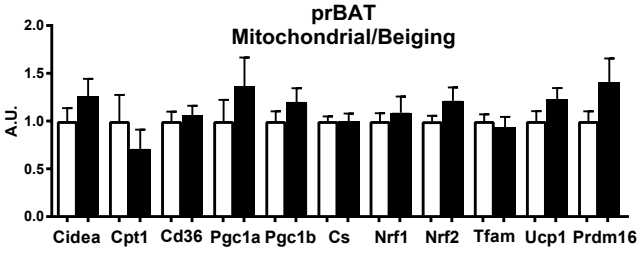
D
prBAT
Mitochondrial/Beiging
A.U.
Cidea Cpt1 Cd36 Pgc1a Pgc1b Cs Nrf1 Nrf2 Tfam Ucp1 Prdm16

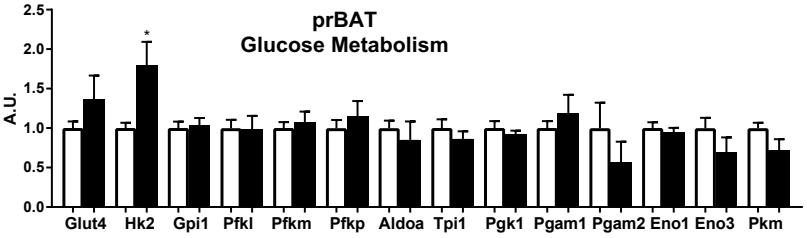
E
prBAT
Glucose Metabolism
A.U.
*
Glut4 Hk2 Gpi1 Pfkl Pfkm Pfkp Aldoa Tpi1 Pgk1 Pgam1 Pgam2 Eno1 Eno3 Pkm

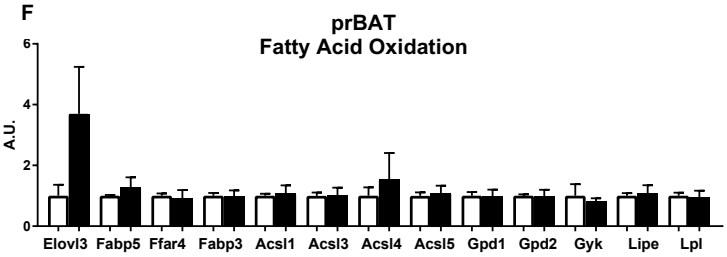
F
prBAT
Fatty Acid Oxidation
A.U.
Elovl3 Fabp5 Ffar4 Fabp3 Acsl1 Acsl3 Acsl4 Acsl5 Gpd1 Gpd2 Gyk Lipe Lpl

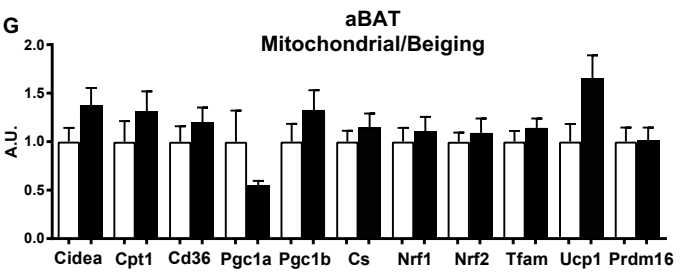
G
aBAT
Mitochondrial/Beiging
A.U.
Cidea Cpt1 Cd36 Pgc1a Pgc1b Cs Nrf1 Nrf2 Tfam Ucp1 Prdm16

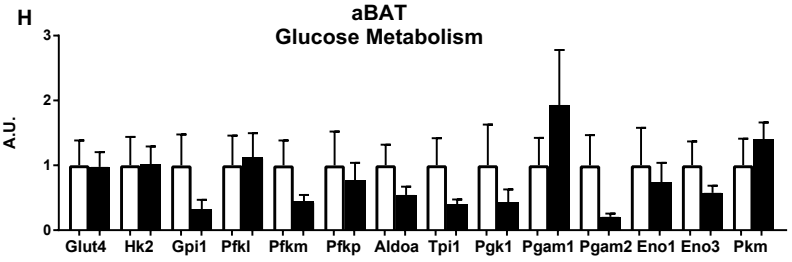
H
aBAT
Glucose Metabolism
A.U.
Glut4 Hk2 Gpi1 Pfkl Pfkm Pfkp Aldoa Tpi1 Pgk1 Pgam1 Pgam2 Eno1 Eno3 Pkm

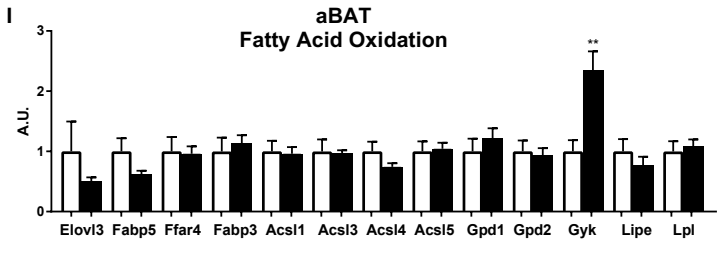
I
aBAT
Fatty Acid Oxidation
A.U.
**
Elovl3 Fabp5 Ffar4 Fabp3 Acsl1 Acsl3 Acsl4 Acsl5 Gpd1 Gpd2 Gyk Lipe Lpl

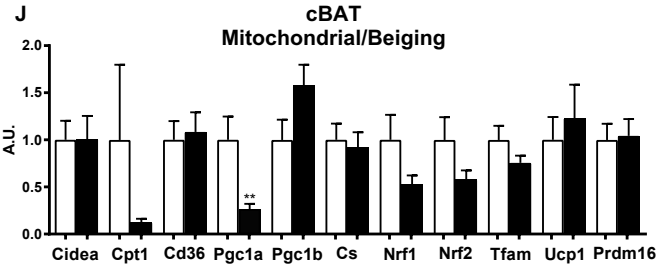
J
cBAT
Mitochondrial/Beiging
A.U.
2.0
1.5
1.0
0.5
0.0
**
Cidea
Cpt1
Cd36
Pgc1a
Pgc1b
Cs
Nrf1
Nrf2
Tfam
Ucp1
Prdm16

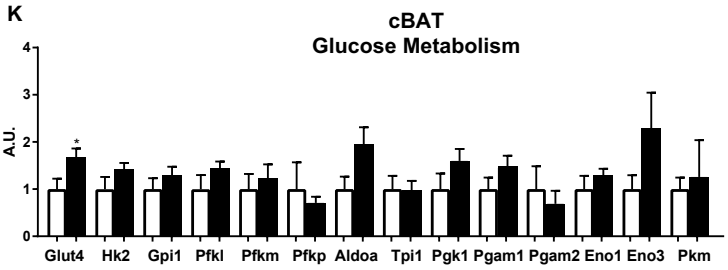
K
cBAT
Glucose Metabolism
A.U.
4
3
2
1
0
*
Glut4
Hk2
Gpi1
Pfkl
Pfkm
Pfkp
Aldoa
Tpi1
Pgk1
Pgam1
Pgam2
Eno1
Eno3
Pkm

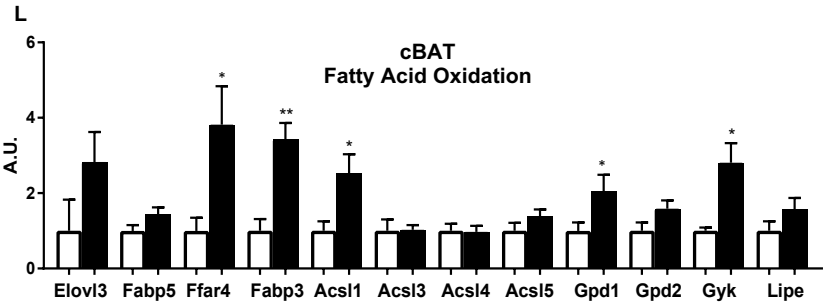
L
cBAT
Fatty Acid Oxidation
A.U.
6
4
2
0
*
**
*
*
*
Elovl3
Fabp5
Ffar4
Fabp3
Acsl1
Acsl3
Acsl4
Acsl5
Gpd1
Gpd2
Gyk
Lipe

Supplementary Table 1: qPCR forward and reverse primer sequences for the genes measured, Related to Figure 2-7.

Gene	Forward Primer Sequence	Reverse Primer Sequence
Cidea	GGTGGACACAGAGGAGTTCTTTC	CGAAGGTGACTCTGGCTATTCC
Cpt1	AAAGATCAATCGGACCCTAGACA	CAG CGA GTA GCG CAT AGT CA
Cd36	TGG AGC TGT TAT TGG TGC AG	TGG GTT TTG CAC ATC AAA GA
Pgc1a	GAATCAAGCCACTACAGACACCG	CATCCCTCTTGAGCCTTTCGTG
Pgc1b	TCCTGTAAAAGCCCGGAGTAT	GCTCTGGTAGGGGCAGTGA
Cs	GACTACATCTGGAACACACTCAATTCA	CGAGGGTCAGTCTTCCTCAGTAC
Nrf1	CAACAGGGAAGAAACGGAAA	GCACCACATTCTCCAAAGGT
Nrf2	AGGTTGCCCACATTCCCAAACAAG	TTGCTCCATGTCCTGCTCTATGCT
Tfam	GTCCATAGGCACCGTATTGC	CCCATGCTGGAAAAACACTT
Ucp1	AGGCTTCCAGTACCATTAGGT	CTGAGTGAGGCAAAGCTGATTT
Prdm16	ATCCACAGCACGGGTGAAGCCAT	ACATCTGCCCACAGTCCTTGCA
Glut4	ATCATCCGGAACCTGGAGG	CGGTCAGGCGCTTTAGACTC
Hk2	AGAGAACAAGGGCGAGGAG	GGAAGCGGACATCACAATC
Gpi1	ATGGGCATATTCTGGTGGAC	CCCGATTCTCGGTGTAGTTG
Pfkl	CCATCAGCAACAATGTGCCTGG	TGAGGCTGACTGCTTGATGCGA
Pfkm	CTGGTGCTGAGGAATGAGAA	TTCCTGTCAAAGGGAGTTGG
Pfkp	AAGCTATCGGTGTCCTGACC	TCCCACCCACTTGCAGAAT
Aldoa	GCGACCACCATGTCTATCTG	GAAAGTGACCCCAGTGACAG
Tpi1	TATGGAGGTTCTGTGACTGGA	CGGTGGGAGCAGTTACTAAA
Pgk1	GAGCCTCACTGTCCAAACTA	CTTTAGCGCCTCCCAAGATA
Pgam1	GACGATCTTATGATGTCCCACC	GTACCTGCGATCCTTGCTGA
Pgam2	CTGCCTACCTGTGAAAGTCTC	GACATCCCTTCCAGATGTTT
Eno1	CTTGCTTTGCAGCGATCCTA	GAAGAGACCTTTTGCGGTGT
Eno3	CTGTGCCTGCCTTTAATGTG	CTTCCCATACTTGGCCTTGA
Pkm	CTGTGGAGATGCTGAAGGAG	CAACAGGACGGTAGAGAATGG
Elovl3	GTGCTTTGCCATCTACACGGATG	ATGAGTGGACGCTTACGCAGGA
Fabp5	GACGACTGTGTTCTCTTGTAACC	TGTTATCGTGCTCTCCTTCCCG
Ffar4	GTGACTTTGAACTTCCTGGTGCC	CAGAGTATGCCAAGCTCAGCGT
Fabp3	AGAGTTCGACGAGGTGACAGCA	TTGTCTCCTGCCCGTTCCACTT
Acsl1	ACACTTCCTTGAAGCGATGG	GGCTCGACTGTATCTTGTGG
Acsl3	GGCCAACGTGGAAAAGAAAG	GTCTTGGAATCCTTCTCGCC
Acsl4	GCACCTTCGACTCAGATCAC	CCAGGTTTGTCTGAAGTGGG
Acsl5	CGCCCCCATCTCCACTCCAG	GCTTCAAACACCCAACATCCCATTGC
Gpd1	CTCATCACGACCTGCTATGG	CTGCTCAATGGACTTTCCAG
Gpd2	GCGGACTCATCACAATAGCA	TGAAGGAACAGCCCAACAG
Gyk	CAAATGCAAGCAGGACGATG	GGCCCCAGCTTTCATTAGG

Lipe	TGGCACACCATTTTGACCTG	TTGCGGTTAGAAGCCACATAG
Lpl	GATGCCCTACAAAGTGTTCCA	AAATCTCGAAGGCCTGGTTG

Transparent Methods

Animals

Male 10-week-old C57BL/6 mice from Charles River Laboratory were fed a chow diet (21% kcal from fat; PharmaServ9f5020) and housed at room temperature (22°C) on a 12-hour light/dark cycle. All procedures were approved by the IACUC at The Ohio State University and the Joslin Diabetes Center.

Mouse Training Protocol

Mice were divided into two groups: sedentary and exercise-trained. The exercise-trained group was individually housed in wheel cages (24.5 cm in diameter and 8 cm in width; Nalgene), allowing for voluntary access to physical activity *ad lib*. The total number of wheel cage revolutions was monitored daily and the accumulated running distance was calculated. Mice were investigated after either 5 or 11 days of exercise training for NADH autofluorscence experiments or after 3 weeks of exercise training for all other experiments. Mice ran an average of 7±0.6 km/day or a total of a 35±1.1km over 5 days, 77±2.7km over 11 days, and or a total of 152±7km over a 3 wk period. Any mouse that ran 10% less than the average of the trained group was excluded from analyses. The sedentary control mice were age-matched and maintained in individual static cages without running wheels and treated identically to the wheel cage–housed mice. After 3 weeks, mice were fasted overnight, removed from the cages, anesthetized 4 hours following removal from static or wheel cage, sacrificed, and all 14 adipose depots (ingWAT, pgWAT, iBAT, mWAT, rpWAT, triWAT, asWAT, prWAT, prBAT, mBAT, cBAT, cWAT, isWAT, and aBAT) were immediately removed, flash frozen in LN_2, and then stored at -80°C.

qPCR

Tissue processing and qPCR were performed as previously described (Lessard et al., 2013). Sigma-Aldrich custom primers were used for genes of interest with the sequences shown in Supplementary Table 1. All qPCR gene expression was normalized to the housekeeping gene GAPDH.

Glucose Uptake in Isolated SVF Differentiated into Adipocytes.

The stromal vascular fraction (SVF) was isolated from ingWAT and iBAT from sedentary and trained mice and was plated at equal cell number. The cells underwent adipogenic differentiation (Stanford et al., 2015; Tseng et al., 2004), and 8 days post-differentiation cells were serum starved for 3 hours in low glucose DMEM. Glucose uptake was determined by the addition of [^{3}H]-2-deoxyglucose for 10 minutes on ice. Cells were washed with ice-cold saline solution and harvested in 0.05 N NaOH to determine net accumulation of [^{3}H]-2-deoxyglucose.

Oxygen Consumption Rates

Isolated SVF from ingWAT, pgWAT, and iBAT were seeded onto gelatin coated 24 well plates and differentiated according to standard protocols. The cell plates and assay cartridges have four ports allowing for drug delivery to individual wells during measurement of oxygen consumption. Cells were serum starved for 1 hour, and oxygen consumption rates (OCR) were measured in media containing 200μM palmitate plus 100μM albumin in a Seahorse XF24 instrument using the standard protocol of 3 minute mix, 2 minute wait, and 3 minute measure. For the bioenergetic profile, cells were first given oligomycin to block ATP synthase, FCCP as an uncoupler, and Rotenone to block Complex 1 of the ETC (all from Sigma).

NADH Autofluorescence and Image Analysis

After 5 and 11 days of exercise training, mice were anesthetized with Phenobarbital sodium (90 mg/Kg, i.p.) and the skin covering the ingWAT or iBAT was opened to expose the AT. The mice were mounted on their side or dorsally in dental cement, as previously described (Lauritzen et al., 2008; Lauritzen et al., 2006). This was followed by 40 minutes of temperature and movement stabilization period with mice placed on a heating pad to maintain core body temperature. After 40 minutes, basal pairs of images were obtained. The Zeiss Chameleon Multiphoton laser was used at 710 nm for excitation of NADH. NADH fluorescence was collected and descanned between 410-650 nm as previously described (Huang et al., 2002). Adipose tissue sections were obtained as TIF images with the Zeiss confocal software and were imported into Metamorph Software (V. 6.1, Universal Imaging Corp). Image stacks were created. The average area and intensity of NADH positive structures were quantified .

Western Blotting

Tissue processing and immunoblotting were performed as previously described (Stanford et al., 2015). The GLUT1, GLUT4, and CD36 (ThermoScientific), FATP1 (Santa Cruz), hexokinase 2 (HK2), citrate synthase (CS) and UCP1 (AbCam), HSL and pHSL(Ser565) (Cell Signaling), and GAPDH (Pierce) antibodies were obtained from a commercial source. All data was normalized to GAPDH antibody.

Statistics

The data are presented as the mean ± SEM. Statistical significance was defined as $p < 0.05$ and determined by two-way Student t-tests. For Seahorse data, all plots represent 8–10

wells per time point per treatment group, and error bars are standard error of the mean (SEM). Quantifications in bar plots are averages of four timepoints with 8–10 wells per time point, and error bars are SEM. Statistical comparisons were done by Student's *t*-test. The number of samples used to determine statistical significance is indicated in the figure legends.

References

Huang, S., Heikal, A.A., and Webb, W.W. (2002). Two-photon fluorescence spectroscopy and microscopy of NAD(P)H and flavoprotein. Biophysical journal *82*, 2811-2825.

Lauritzen, H.P., Galbo, H., Brandauer, J., Goodyear, L.J., and Ploug, T. (2008). Large GLUT4 vesicles are stationary while locally and reversibly depleted during transient insulin stimulation of skeletal muscle of living mice: imaging analysis of GLUT4-enhanced green fluorescent protein vesicle dynamics. Diabetes *57*, 315-324.

Lauritzen, H.P., Ploug, T., Prats, C., Tavare, J.M., and Galbo, H. (2006). Imaging of insulin signaling in skeletal muscle of living mice shows major role of T-tubules. Diabetes *55*, 1300-1306.

Lessard, S.J., Rivas, D.A., Alves-Wagner, A.B., Hirshman, M.F., Gallagher, I.J., Constantin-Teodosiu, D., Atkins, R., Greenhaff, P.L., Qi, N.R., Gustafsson, T., et al. (2013). Resistance to aerobic exercise training causes metabolic dysfunction and reveals novel exercise-regulated signaling networks. Diabetes *62*, 2717-2727.

Stanford, K.I., Middelbeek, R.J., Townsend, K.L., Lee, M.Y., Takahashi, H., So, K., Hitchcox, K.M., Markan, K.R., Hellbach, K., Hirshman, M.F., et al. (2015). A novel role for subcutaneous adipose tissue in exercise-induced improvements in glucose homeostasis. Diabetes *64*, 2002-2014.

Tseng, Y.H., Kriauciunas, K.M., Kokkotou, E., and Kahn, C.R. (2004). Differential roles of insulin receptor substrates in brown adipocyte differentiation. Molecular and cellular biology *24*, 1918-1929.